



Nanobubbles and the hydrophobic attraction

Phil Attard*

Australian Research Council, University of South Australia, Mawson Lakes, SA 5095, Australia

Abstract

The evidence for nanobubbles as the origin of the long-ranged attractions measured between hydrophobic surfaces immersed in water is reviewed by focusing upon several unique features of the force curves. Also covered is the morphology of nanobubbles as revealed by direct imaging with tapping mode atomic force microscopy. A discussion of the origin, thermodynamic stability and practical implications of nanobubbles is given.

© 2003 Elsevier Science B.V. All rights reserved.

Keywords: Nanobubble; Hydrophobic attraction; Surface force; Force measurement

1. Introduction

The famous DLVO theory—named for Derjaguin, Landau, Verwey and Overbeek—describes the stability of a colloid dispersion as a balance between the electric double layer repulsion and the van der Waals attraction. The range of the former may be 1–100 nm, scaling inversely with the square root of the ionic strength, and the measurable or effective range of the latter is practically 1 nm or so. In addition to these there may be polymer bridging or depletion forces that extend to the radius of gyration of the polymer, and solvation or structural forces whose extent is not more than several molecular diameters. These four forces underpin colloid science, and the quantitative understanding of their molecular basis has led to their widespread control and exploitation.

The long-ranged attractions, measurable up to several hundred nanometers, between hydrophobic or water repellent surfaces do not fit in to any of these categories, and they have been the subject of much interest and speculation. Initial

*Present address: School of Chemistry F11, University of Sydney, NSW 2006, Australia. Tel.: +61-2-9351-5878; fax: +61-2-9351-3329.

E-mail address: p.attard@chem.usyd.edu.au (P. Attard).

evidence came from the large separations at which bubbles ruptured approaching a hydrophobic substrate [1], and from direct force measurements [2,3]. In the ensuing years, experiments were performed in many laboratories on a variety of hydrophobic surfaces. These broadly confirmed the existence of the attraction, although there was some variability and certain contradictions in the detail of the measurements, and there lacked a compelling theory for the origins of the force. Nevertheless, by the end of the 20th century consensus had emerged that a fundamentally new and important force had been discovered. Christenson and Claesson have reviewed the experimental situation to 1999 [4].

2. Theoretical review

There has been a wide ranging debate about the origins of this hydrophobic attraction. Four theories have been explored in some detail: (i) solvent structuring; (ii) electrostatic correlations; (iii) approach to a spinodal separation; and (iv) bridging nanobubbles. Besides these theories a number of other ideas have been put forward that have not been widely taken up due to either a lack of experimental support or else to uncertainty about the validity or applicability of the approach.

- i. An early theory attributes the long-ranged hydrophobic attraction to surface-induced solvent structure propagating between the two surfaces [5]. The difficulty with this idea is that simulation and other evidence show that the change in the structure of a liquid near a surface only persists for several molecular diameters and beyond that the liquid is essentially indistinguishable from the disordered bulk. Since the hydrophobic attraction has been measured at separations corresponding to hundreds, or even thousands of molecular diameters, it cannot be accounted for by surface-induced structure. Also, the long-range hydrophobic attraction has been measured in solvents other than water [6], and one can conclude that the attraction has little to do with the cooperativity or associativity of water. This propagating structure mechanism is undoubtedly the origin of the interaction between apolar molecules and the tertiary structure of hydrophobic macromolecular moieties, which phenomena are also commonly known as hydrophobic interactions, but it is unrelated to the attraction measured at large separations between macroscopic hydrophobic surfaces. The term ‘hydrophobic attraction’ is used herein to refer exclusively to the latter.
- ii. Another early theory asserts that the attraction is due to electrostatic correlations [7], a form of zero frequency van der Waals force with an anomalous electrostatic response induced by the surfaces. Solvent [7] and electrolyte [8,9] fluctuations and correlated charge domains [10–12] have all been analysed. A very strong prediction of the theory is that the attraction should be exponentially decaying at a rate equal to half the Debye length. Whilst there is some experimental data that is consistent with this result [3,13–16], more recent and detailed experimental tests have shown that the force is largely independent of ionic strength and is measurable even at molar electrolyte concentrations [17–22]. This conclusively rules out any electrostatic mechanism in those particular systems. Also, the long-

ranged attraction has been measured between solvophobic surfaces in non-polar liquids [6], which is also evidence against an electrostatic mechanism.

- iii. A more esoteric theory is based upon the existence of long range correlations in a near-critical or near spinodal bulk fluid, and it proposes that the attraction is due to the separation-induced cavitation and density depression in a liquid confined between solvophobic walls [23]. The relevance to the hydrophobic attraction follows from the experimental observation of hysteresis in the force measured between hydrophobic surfaces upon approach and retraction. The water between the surfaces cavitates once they are brought into contact, and the vapour cavity persists bridging the surfaces until they are separated by hundreds of nanometers [3,19,20,24]. A simple thermodynamic calculation shows that for surfaces with a contact angle greater than 90° , such a vapour bridge is stable with respect to the liquid out to large (hundreds of nanometers) separations [23]. Since cavitation is not observed on approach prior to the jump into contact, the aqueous interlayer must be in a metastable state, and the question arises as to whether there exists a spinodal separation below which it is impossible to prevent the water cavitating. The significance of such a spinodal is that the forces between particles are predicted to be universally long ranged and attractive approaching the bulk critical point or bulk line of spinodal composition [25,26]. Hence, in connection with the long-range hydrophobic attraction, it has been proposed that such long-ranged attractions would also exist prior to separation-induced spinodal cavitation [23]. This idea was explored by grand canonical Monte Carlo simulations of a Lennard–Jones fluid between hard-walls, and it was shown indeed that the liquid does cavitate at small separations, that there is hysteresis between approach and retraction and that on the metastable liquid branch, on approach, the density is increasingly depressed and the force is increasingly attractive as the spinodal separation is approached [23]. These results have been subsequently confirmed by other calculations [27–29], although in some cases, the calculated attractions are for the case that a vapour cavity has already been induced. This contradicts the experimental evidence that the cavitation only occurs at contact or upon separation from contact, which is of course after the onset of the long-ranged attraction. The long-ranged attractions in a bulk near-critical and near-spinodal fluid are an incontrovertible fact for which there is both theoretical [25,26,30,31] and experimental [32–34] evidence. However, the simulations of separation-induced cavitation yield length scales for the attraction that are less than some 10 molecular diameters [23], which is too short to account for the measured hydrophobic attraction.
- iv. A final theory, and the one that is the focus of this review, proposes that sub-microscopic bubbles, (nanobubbles), preexist on the hydrophobic surfaces and that it is their bridging that gives rise to the measured forces [19,35]. There are many attractive features of this idea, not least of which is that the range of the force is essentially set by the bubble size, and so one can avoid having to invoke some long-range mechanism by which the presence of one surface is communicated to the other through the aqueous interlayer. As is discussed in detail below,

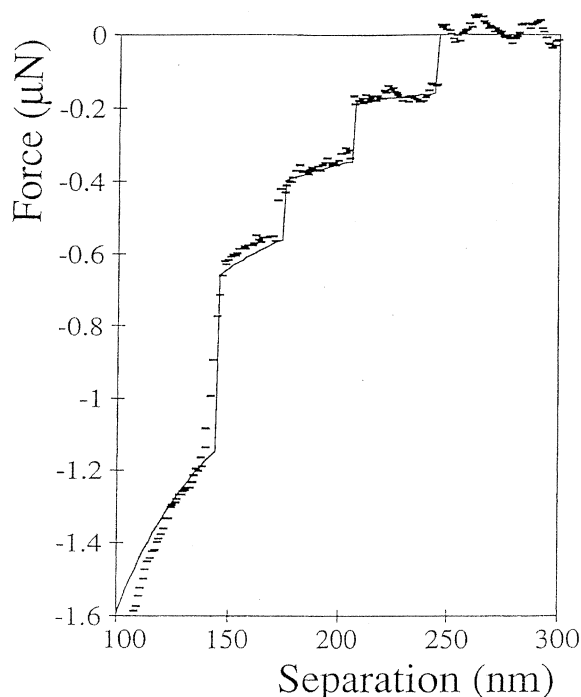


Fig. 1. The steps in the attractive force at long range measured between macroscopic, (radius 2 mm), hydrophobic surfaces in water that led to the original idea that nanobubbles exist on such surfaces and that their bridging is responsible for the hydrophobic attraction. The line is a thermodynamic calculation of the force fitted with six bridging bubbles. Reproduced with permission from Ref. [19]. Copyright 1994 Am. Chem. Soc.

the theory appears capable of reconciling much of the experimental data and of explaining many of the features of the force measurements. The indirect evidence from force measurements is complemented by direct scanning probe images of the nanobubbles, and their size and shape are discussed in Section 4. The main difficulty with the proposal is to account for the apparent stability of the nanobubbles, and the relevant considerations are critically assessed in Section 5. A summary and brief discussion of possible applications concludes the review.

3. Evidence from force measurement

The idea that nanobubbles are responsible for the measured long-ranged attraction between hydrophobic surfaces was originally based upon the observation of steps in the force data [19]. Fig. 1 is taken from the original paper and it shows the attractive force measured between two hydrophobic surfaces, (silanated glass, 2-mm radius), in water [19]. These data were obtained with the MASIF device, which has a higher resolution and a greater density of data points than earlier surface force

measurements. The new measurements revealed steps or discontinuities in the force at large separations. Each step was taken to represent the attachment to the approaching surface of a bubble already on the apposite surface. The bubbles were argued to have originated during the immersion of the surfaces in the water or to have nucleated from the solution that had become supersaturated with air [35]. The radius of the bubbles may be assumed to equal the separation at which they bridged, (but see images below), and the fact that this is less than a micron accounts for the inability to observe them optically. After bridging the bubble grows laterally, driven by the favourable replacement of solid–water with solid–vapour contact, and this gives rise to the measured attraction.

The observation of steps provides indirect evidence for nanobubbles, but on its own it is perhaps not entirely convincing since one could possibly imagine a number of alternative explanations. However, a thermodynamic analysis of the force due to a bridging bubble can account quantitatively for the measured force [19]. It can be seen in Fig. 1 that the force is fitted in detail by a thermodynamic calculation involving six bridging bubbles of radius 300 nm placed strategically off the central axis.

Despite the evident consonance of theory and experiment shown in Fig. 1, initially the nanobubble hypothesis was not widely accepted. The main objection is that bubbles with a radius of curvature of 10–100 nm should, by the Laplace–Young equation, have an internal gas pressure of hundreds or tens of atmospheres and it is argued that they should dissolve within milliseconds [36,37]. This objection was in fact anticipated by the original authors [19,35], who concluded that since the experimental evidence for the nanobubbles is so compelling, the paradox can only be resolved by asserting that the bubbles are not in equilibrium with the atmosphere due to the rather long time it takes to reach diffusive equilibrium. This issue is addressed below in Section 5 on the thermodynamic stability of nanobubbles.

Two experimental lines of enquiry have bolstered the case for nanobubbles as the origin of the hydrophobic attraction. First have been force measurements, where an attempt has been made to control the amount of dissolved air in solution, and hence, presumably, the nanobubbles themselves. A number of such measurement in de-aerated water have been performed [20,38–41]. The general conclusion is that the force is more short ranged in degassed water than in water exposed to the atmosphere. The experiments are not entirely conclusive because the attraction does not completely vanish in de-aerated water, and it appears difficult to completely isolate the force measurement cell from the atmosphere or to guarantee that the solution is entirely free from air. Nevertheless, in view of their own and other results, Wood and Sharma [20] argue that a source of the nanobubbles is the passage of the surfaces through the air–water interface since surfaces hydrophobed in situ under water tend to display more short-ranged attractions than those prepared in air prior to transfer to water.

The second experiment, and the one that has probably played the major role in leading a consensus, were force measurements performed with the atomic force microscope (AFM) by Carambassis et al. [22]. Fig. 2 shows the results of AFM

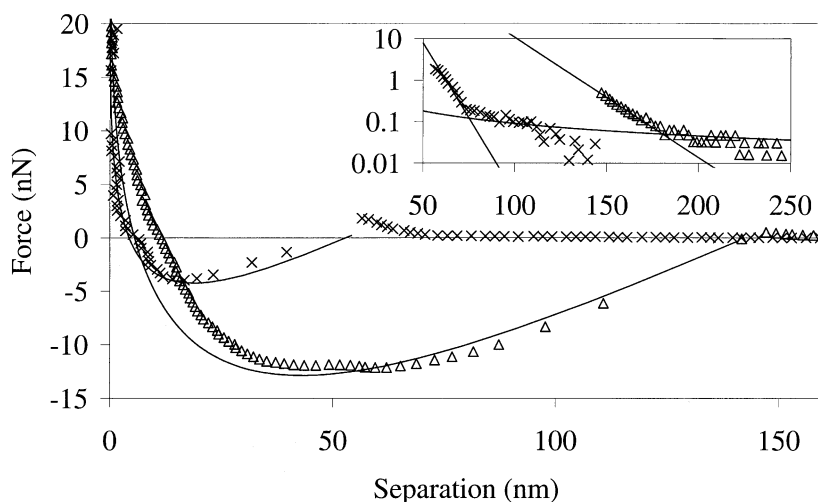


Fig. 2. Two measurements of the force between hydrophobic surfaces showing the attraction at large separations, the pre-jump repulsion and the soft post-jump repulsion approaching contact [22]. The curves in the main figure are the calculated force due to a bridging bubble, (original radii 75 and 200 nm), that spreads with a drag coefficient of 20 kNsm^{-2} [42]. In the inset the pre-jump repulsion is magnified on logarithmic scale, with the flat curve being the calculated hydrodynamic drainage and the steeper straight line being an exponential fit to the data (decay lengths 15 and 6 nm).

measurements between a glass sphere and an oxidised silicon wafer, both hydrophobed with dichlorosilane to give a contact angle greater than 100° [22]. Three points are noticeable in the data: (i) the variability in the distance of the jump into contact; (ii) the steep repulsion prior to the onset of the attractive jump; and (iii) the gradual increase in the repulsion after the jump coming into contact (soft compliance).

- i. Conventional surface forces are quite reproducible, but not so for the long-ranged attractions between hydrophobic surfaces, as shown by the results of Carambassis et al. [22]. The variability in the forces shown in Fig. 2, (which also occurs in measurements at the same electrolyte concentration), can be rationalised if the attraction is due to bridging nanobubbles and the difference in jump distance reflects different sized bubbles. In some cases, no jump or long-range attraction is seen, which can be understood if there are no nanobubbles present in the contact region.
- ii. The steep repulsion prior to the attractive jump decays too rapidly to have originated between the substrate and the probe, and one concludes that it must be due to the interaction with an object of height equal to the jump distance protruding from one of the surfaces. The fact that this object subsequently disappears upon the jump into solid–solid contact provides strong evidence that the object is a nanobubble. Furthermore, the existence of a repulsion indicates that the nanobubble was already on the surface prior to the approach of the second surface. If the jump were due to cavitation induced by the approaching

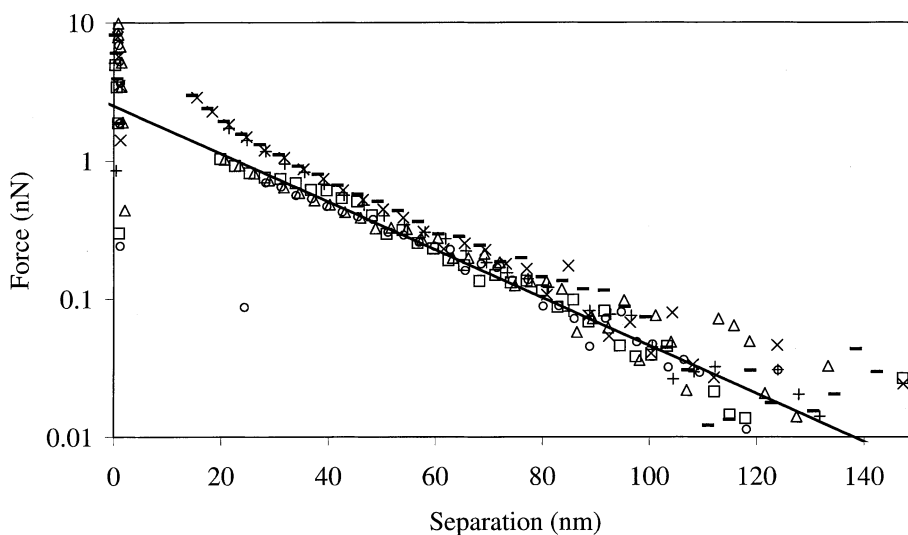


Fig. 3. The pre-jump repulsion on a logarithmic scale [45]. The characters are pH 9.4 and the symbols are pH 5.6, there is no added electrolyte and the driving velocities are 0.2–13.8 $\mu\text{m/s}$. The straight line has decay length of 25 nm.

probe, then there would be a monotonic attraction without the repulsion. This prejump repulsion is perhaps the most unambiguous signal of nanobubbles and it has since been confirmed by a number of workers [39–41,43–45]. The decay lengths for the pre-jump repulsion in Fig. 2 are 15 and 6 nm, to be compared with respective Debye lengths of 22 and 3 nm for the 0.19 and 9.5 mM NaCl solutions in which the measurements are performed. Fig. 3 shows this repulsion measured at different pH and different driving velocities, but with no added electrolyte [45]. Again the decay length, in this case 25 nm, is much shorter than the Debye length, (192 and 61 nm at these pH), and it is independent of pH and driving velocity. From the last fact, one can conclude that that the repulsion is not a hydrodynamic effect, (although the jump-in distance tends to decrease with increasing speed [45]). It cannot be a traditional electric double layer repulsion because of the decay length, but the fact that the magnitude of the force increases with increasing pH indicates that charge does play a role. This is supported by the fact that the repulsion is absent at pH 3 [45], which turns out to be the point of zero charge of the air–water interface [46,47]. This itself is of course strong evidence for the interpretation of the repulsion as signifying the interaction with nanobubbles protruding from the surface. The most likely explanation for fact that the decay length does not equal the Debye length is that the surface is heterogeneous and rough due to multiple nanobubbles in the interaction region (see images below). For such heterogeneous double layers, the decay length at separations less than 1 Debye length is determined by the length scale of the heterogeneity [48].

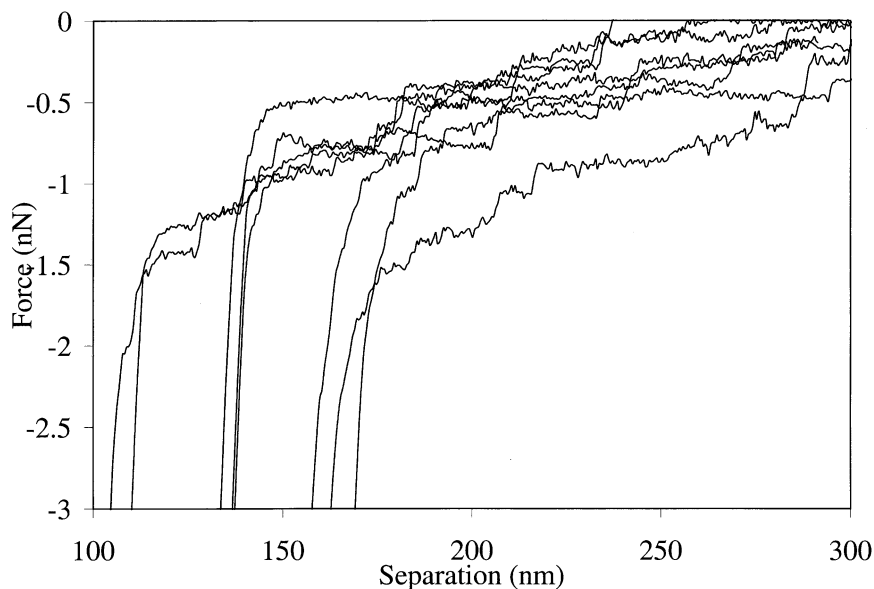


Fig. 4. Steps in the retraction force curve following the hydrophobic surfaces jumping out of contact [45].

iii. The soft compliance or hook region approaching final contact is also quite unusual in the context of normal surface forces, but it can be understood as a dynamic effect due to the finite rate of lateral spreading of the bridging nanobubble [22,42]. Fig. 2 shows that the region is quite well fit by a theoretical calculation based upon a constrained entropy approach [49,50], but taking into account the drag on the moving contact line. Whilst the force due to an equilibrium bridging bubble, (i.e. one in which the lateral radius is optimum at each separation), is always attractive, the force due to a steadily expanding bubble, (i.e. one in which the contact line drag is balanced by the thermodynamic expansion force) turns repulsive at small separations as the air inside the suboptimal bubble is compressed. The thermodynamic calculations were carried out at fixed number of gas molecules rather than at fixed gas chemical potential, the rationale being that the existence of nanobubbles implies that the gas is not in diffusive equilibrium with the atmosphere [19,35,42]. The fact that the measurements show this soft compliance regime due to the compression of the bubble vindicates this approach, at least on the time scales of the measurements, since the soft repulsion would not be present if the gas could dissolve into the solution.

The final piece of force evidence for nanobubbles comes from adhesion or pull-off force measurements. Whereas normal adhesive surfaces jump directly from contact to zero force, in the case of hydrophobic surfaces they jump to a weak,

almost flat, attractive force and approach zero in discrete steps [41,45]. Examples are shown in Fig. 4 [45]. For the case of bridging nanobubbles, thermodynamic calculations show that there are two local minima in the lateral size of the equilibrium bubble: at small separations the bridging bubble is of microscopic lateral size; and at large separations it is of submicroscopic dimensions, (i.e. it is very long and thin) [42]. On the latter branch the force is weak, attractive and slowly varying, just as on each step in Fig. 4. The interpretation of the data are that following the jump out of contact the microscopic bridging bubble collapses into multiple submicroscopic bridging bubbles and the snapping of each of these gives rise to the steps in the force. It is worth mentioning that such multistranded, thin, bridging bubbles have been observed visually in the surface forces apparatus after the vapour cavity between the hydrophobic surfaces has collapsed following the jump from contact [24].

One difficulty with the nanobubble interpretation of the data in Fig. 4 is the value of the pull-off force, which is in the range 50–100 nN. For a sphere of radius $R = 7.5 \mu\text{m}$, the capillary adhesion is expected to be $F = 4\pi R\gamma\cos\theta$, or 1200 nN for a contact angle of 100° (both surfaces). It would require a contact angle of 91° , (both surfaces), or contact angles of 100° on one surface and 81° on the other, to reduce this to the measured value. These seem unrealistically low, and a more likely explanation is that the AFM is underestimating the adhesion due to the cantilever rolling and twisting during the pull-off.

4. Images of nanobubbles

The force-based evidence for nanobubbles as the origin of the hydrophobic attraction is necessarily indirect; their presence can be inferred from the details of the force curves, but their nature is not explicitly evident. Their putative submicron size makes optical visualisation impossible, but nevertheless, attempts have been made to use scanning probe methods to image them. Fig. 5 shows tapping mode images of silanated glass surfaces, (rms roughness less than 0.5 nm), in water [44,45]. The images are from the same series of experiments as the force measurements in Fig. 3. What is most surprising about the images is that they reveal the nanobubbles to be irregularly shaped and to form a close-packed, almost interconnected network that virtually covers the surface with a film of gas. Prior to these images most workers had imagined the nanobubbles as isolated hemispherical objects sparsely distributed on the hydrophobic surfaces. The contrary morphology and density revealed in Fig. 5 offers insight into the origin and the stability of the nanobubbles that is obscured by the naive expectation, as is discussed below.

The evidence that the features in Fig. 5 indeed represent nanobubbles comes from the phase images, which show that the features are composed of a softer material than the substrate. Furthermore, contact mode imaging of the substrate in water with a relatively large applied load show it to be smooth, ($<0.5 \text{ nm}$ rms roughness), and featureless, which indicates that the features have been scraped aside and destroyed. Tapping mode images obtained within approximately 20 min of completing the contact mode scan show that the nanobubbles had re-emerged virtually

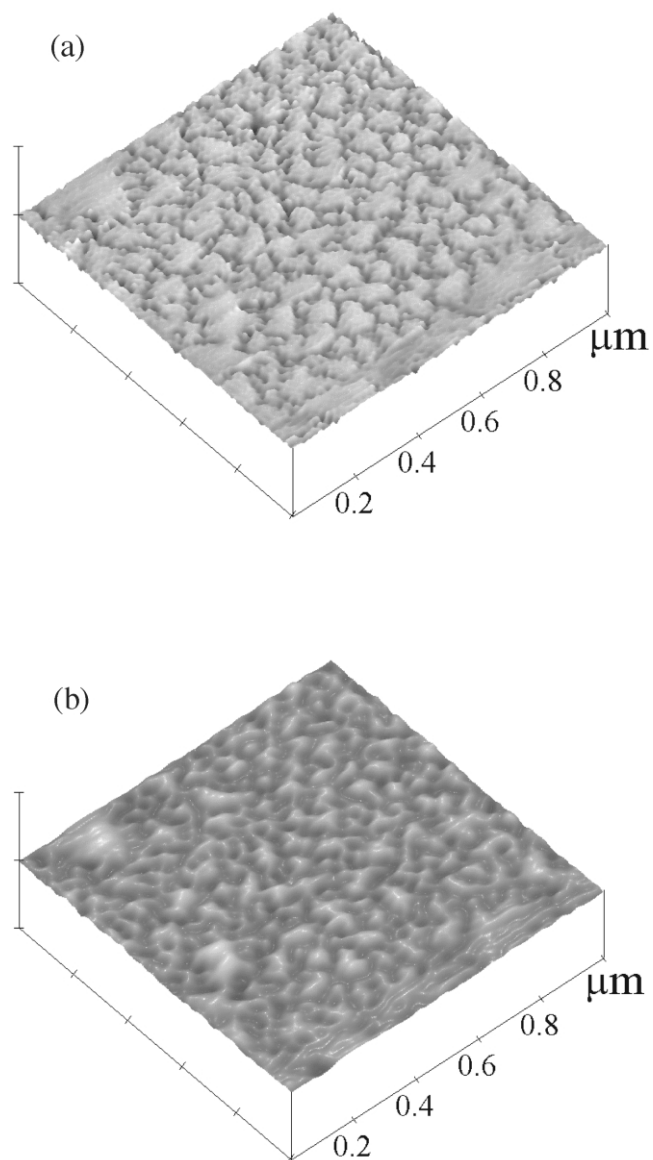


Fig. 5. Phase, [(a) 10° valley to peak], and height, [(b) 30-nm valley to peak], scanning probe tapping mode images of hydrophobic surfaces in water at pH 5.6. The light areas are interpreted as nanobubbles. Reprinted with permission from Ref. [44]. Copyright 2001, Am. Phys. Soc.

unchanged [44,45]. Further experiments were performed to confirm the growth and disappearance of the nanobubbles by flushing the fluid cell and performing measurements in water, then ethanol, then water again [45]. The silanated substrate

is lyophilic for ethanol, with a contact angle of 29° and it is lyophobic, (hydrophobic), for water, with a contact angle of 101° . In water, immediately preceding and immediately succeeding the ethanol, the surfaces showed an attractive jump into contact, a strong adhesion and nanobubbles were imaged in tapping mode. However, in the intervening measurements in ethanol there was no attraction, no adhesion and the tapping mode images were featureless [45]. This is of course consistent with conclusion from the contact angle measurements that it is favourable for air in the form of nanobubbles to displace water from the substrate but it is unfavourable for them to displace ethanol. Both results, (the featureless images obtained with contact mode in water and with tapping mode in ethanol), confirm that the domains shown in Fig. 5 are not chemical or physical roughness or polymeric species on the substrate induced by the silanation procedure.

It should be mentioned that Ishida et al. have also presented tapping mode images of hydrophobic surfaces [51]. However, the features that they identify as nanobubbles are rather different to those seen by Tyrrell and Attard [44,45]. Ishida et al. [51] observe hemispherical objects of uniform circular cross-section, approximately 0.5–1 μm in diameter. The objects are isolated from each other although there is some grouping and alignment evident, and the surface coverage is quite low. One cannot of course rule out these images as artifactual, since the different nanobubble morphology and density could well represent different solution conditions. The 100% coverage revealed by Tyrrell and Attard [44,45] would be expected to result in every force measurement at every contact positions showing the long-range attraction due to bridging nanobubbles, which was indeed the case in their experiments. In contrast, the earlier work of Carrambassis et al. [22] on the same surfaces but different solution conditions, showed that approximately 5% of force measurements did not display a long-range attraction, which was interpreted as less than 100% coverage of nanobubbles, a conclusion also reached by Parker et al. [19] from the data in Fig. 1.

The nanobubbles exhibited in Fig. 5 are quite irregular. The fact that the nanobubbles are not circular in cross-section indicates that the forces that pin the contact line or that resist its motion are large compared to the surface tension that seeks to minimise the area of the liquid–vapour interface (see Section 5). Although there is obvious variability in the size and shape of the nanobubbles, Fig. 6 shows that to leading order the curvature is relatively uniform, which is the signature of thermodynamic equilibrium. (The radii of the circles fitted to the cross-section generally underestimate the radius of curvature because the normal to the surface of the nanobubble does not necessarily lie in the plane of the cross-section.) Evidently the repulsion between the nanobubbles from the charge on the air–water interface, (cf. the discussion of Fig. 3 above), also increases their curvature: the charged bubbles at pH 5.6 have radii 50–90 nm, [as is also the case for cross-sections taken at pH 4.4 and pH 9.4, (not shown)], whereas the uncharged nanobubbles at pH 3.0 have radii 100–200 nm. Presumably, the more highly charged bubbles are prevented from coalescing and growing laterally.

What is also interesting in Fig. 6 is the decoupling of height from radius. Whereas it had originally been assumed that the separation at which the surfaces jumped into

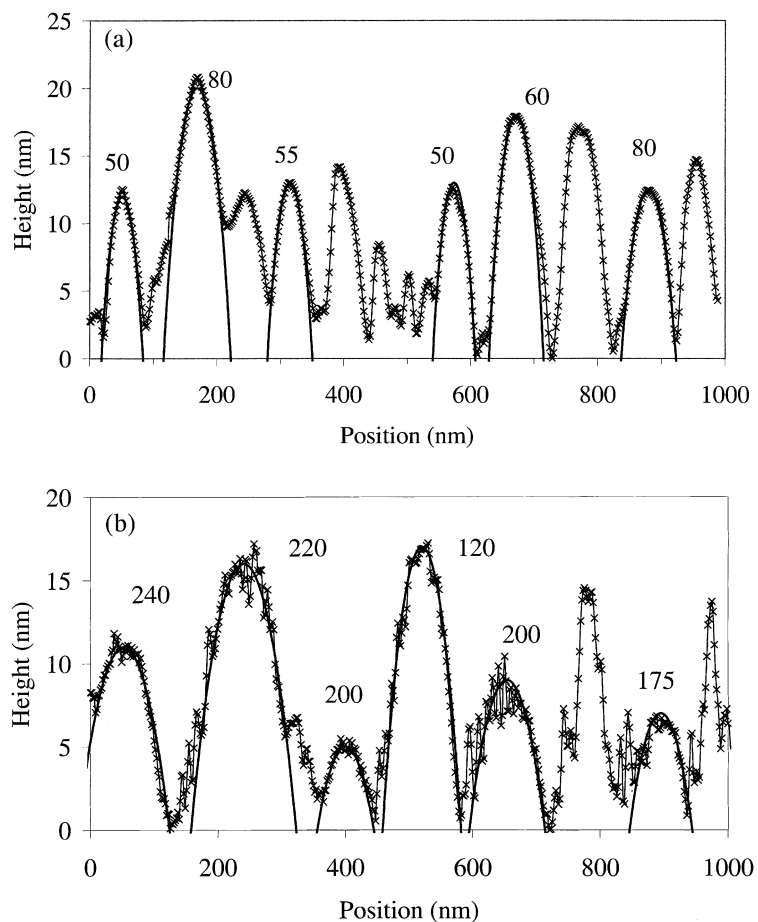


Fig. 6. Cross-section through the tapping mode images at pH 5.6, (a), and at pH 3.0, (b). The symbols are the experimental data [44,45], (taken from Fig. 5a) and the parabolas are actually circles, (note different scales on axes), with in each case the adjacent number being the fitted radius in nanometers.

contact equalled the height of the nanobubbles above the surface, and that this equalled their radius of curvature, the data in Fig. 6 show that their height, (≈ 20 nm), is indeed approximately equal to the position of the jump, (≈ 20 nm, see Fig. 3), and that this is substantially less than the radius of curvature (≈ 50 – 200 nm).

5. Nanobubble stability

One of the major issues that must be faced in ascribing the long-ranged attraction between macroscopic hydrophobic surfaces to bridging nanobubbles is the origin and stability of the nanobubbles. The problem revolves around the Laplace–Young equation:

$$p_{\text{in}} = p_{\text{out}} + \frac{2\gamma}{R}$$

which shows that the pressure inside the nanobubble is greater than that in the solution by an amount proportional to the surface tension of the liquid–vapor interface, $\gamma = 72$ mN/m and inversely proportional to the radius of curvature of the nanobubble. For the 50–80-nm nanobubbles of Fig. 6a this gives an excess pressure of 30–20 at. and for the 100–200-nm nanobubbles of Fig. 6b this gives an excess pressure of 15–7 at.

There appear to be three possible hypotheses for reconciling the experimental evidence for nanobubbles outlined above with the apparently paradoxical Laplace–Young equation: (i) the nanobubbles are not in equilibrium because the times-scales for equilibration are exceedingly long; (ii) the nanobubbles are in equilibrium, but with a supersaturated solution; and (iii) the Laplace–Young equation is not quantitatively applicable.

(i) One can estimate the driving force for equilibration from the chemical potential, which, assuming the gas is ideal, is $\Delta\mu = k_{\text{B}}T \ln[1 + 2\gamma/p_{\text{out}}R]$, where $k_{\text{B}}T$ is the thermal energy. The radii fitted in Fig. 6 correspond to an excess over the atmospheric value of 2–3.4 $k_{\text{B}}T$. This shows that although the bubbles are not in equilibrium with the gas in the atmosphere, the gradient that drives equilibration over the centimeter-sized fluid cell is quite small, being of the order of $10^{-6} k_{\text{B}}T$ per molecular diameter. One might reasonably conclude from this that there is little tendency toward equilibrium and that the nanobubbles would be relatively long-lived.

In contrast, Ljunggren and Eriksson [37], using Fick’s and Henry’s law, calculate quite short lifetimes for nanobubbles, 0.1 ms for a 100-nm radius nanobubble, and their formula predicts a lifetime of less than 1 s for micron-sized bubbles. These estimates seem to contradict the lifetimes of order of at least several tens of minutes implied for the nanobubbles in Fig. 5, and the visual observations of microbubbles by Carambassis et al. [22] and of Considine and Drummond [6], who observed little change over several hours. Given the contradiction between the theoretical calculation and the experimental evidence, one must presume that either Fick’s or Henry’s law is inapplicable at the implied gas concentrations of 0.1–0.01 M, or else that the surface of the nanobubble is providing an impediment to the diffusion of gas across it [see also (iii) below]. It is arguable that the flux across the interface ought to be proportional to the difference between the actual concentration proximal to the interface and that predicted by Henry’s law, which difference is assumed to be zero in the calculations of Ljunggren and Eriksson [37].

(ii) There is some evidence to suggest that the nanobubbles are in equilibrium: (a) the nanobubbles reform in a matter of minutes after being removed or disrupted by: (1) contact mode scraping [44]; (2) flushing with ethanol [45]; and (3) apparent penetration by the tip during tapping mode imaging [45]. (b) The nanobubbles appear to shrink and grow reversibly upon alternately flushing the fluid cell with aerated and deaerated water, as indicated by the change in jump-in distance [39].

(c) All nanobubbles appear to have approximately the same radius of curvature at a given pH, (see Fig. 6) and the radius of curvature reversibly grows (Fig. 6) or shrinks (not shown) by decreasing or increasing the pH. If the nanobubbles were not in some form of equilibrium, or if the equilibration time was long compared to experimental time scales, it would be difficult to account for these phenomena. If the nanobubbles are in equilibrium, then, by the arguments given in the preceding paragraph, [but see also (iii) below], the solution must be supersaturated with air. Sources of air in addition to that originally dissolved by exposure of the water to the atmosphere include: (a) air clinging to the surface during its first passage through the air–water interface [19,20,35,41]; (b) entrapment of air bubbles whilst pumping fluid through the fluid cell; and (c) heating of the originally saturated solution by the AFM laser or piezo-drive or by the surface forces apparatus light bulb. Whilst there does appear to be an activation energy barrier to the initial formation of nanobubbles ([41], Fig. 5), once formed the above arguments for some form of equilibrium holds. In particular, the morphology revealed by Fig. 5 is strongly suggestive of air being driven out of a supersaturated solution.

There are two counter-arguments to this equilibrium with a supersaturated solution viewpoint: (a) the amount of supersaturation for equilibrium seems incredibly large, (0.01 M of air for a 100-nm nanobubble at room temperature); (b) the larger bubbles should grow by cannibalising the smaller bubbles by Ostwald ripening, (although pinning and the electrical double layer repulsion may inhibit their lateral growth [52,53]), and this process should continue until the solution is no longer supersaturated and the interface is planar. An experimental counter-observation to nanobubble equilibrium is that long-range attractions (and hence, presumably nanobubbles) do not completely vanish in de-aerated water [20,38–41].

(iii) The main line of reasoning that would deny the applicability of the Laplace–Young equation focuses upon the surface tension. The latter may be lower than its usual value due to: (a) curvature corrections; (b) adsorption of an insoluble monolayer; and (c) a decrease in surface tension with supersaturation. (a) The first of these may be dismissed because Tolman’s length is of the order of 1 molecular diameter and the surface tension is known to depart significantly from its planar value only for radii of the order of several molecular diameters [54]. (b) Whilst an adsorbed monolayer could reduce the surface tension to ultra-low values, it is difficult to conceive of the origin of the material for such a monolayer for the case of the chemically modified surfaces reviewed in detail here; any unreacted or physisorbed silane would presumably be removed during the washing processes prior to measurement. [Such a putative monolayer presumably would also slow the diffusion of gas across the interface; see (i) above.] (c) Finally, the surface tension of a liquid–vapour interface is known to vanish approaching the bulk critical point or line of spinodal decomposition [55], and one expects similar behaviour for the case of a supersaturated solution [see (ii) above].

There is little direct experimental evidence for such a reduction in surface tension. One could argue that the irregular shapes and cross-sections revealed in Fig. 5 shows that the driving force to minimise the surface area is small compared to the

forces pinning the three-phase line, which is consistent with a reduction in the surface tension. Perhaps one could argue that nanobubbles would be too rigid to give the phase lag evident in Fig. 5a unless the surface tension were significantly less than its usual value. However, the internal pressure of a 10-nm nanobubble with the usual value of surface tension is 1.4×10^7 N/m², which is still more than 1000 times less than Young's modulus for a 'hard' solid.

A further line of enquiry regarding the applicability of the Laplace–Young equation explores the stability of the nanobubbles in the context of the proximity of the solid surface. One possibility may be that the chemical potential of the gas is reduced by van der Waals interactions with the solid. Calculations using reasonable values of the Hamaker constant show this effect to be negligible on the necessary length scales. A second possibility is that there may be some long-range repulsive interaction between the liquid–vapour interface and the surface. In this case, one would expect 'mesa' bubbles with flat tops, not the curved nanobubbles shown in Figs. 5 and 6.

6. Discussion and conclusion

This review of the origin of the long-ranged attractions measured between macroscopic hydrophobic surfaces has focused upon nanobubbles as the most likely explanation. Three possible counter-theories—surface-induced polystructural solvation [5]; electrostatic correlations [7]; and surface-induced density depression and spinodal cavitation [23]—were discussed and the experimental and theoretical evidence against each detailed. Nanobubbles, which were originally proposed by Parker et al. [19], enjoy rather more support and the experimental evidence for them was covered here in the context of force measurement and scanning probe images. In this theory, the measured long-range attraction is attributed to nanobubbles bridging between the two surfaces and drawing them together. Unique features of the force curves that identify nanobubbles as the origin include steps or discontinuities at the moment of attachment [19], extreme variability in the range of the force due to variability in the coverage and size of the nanobubbles [22], a pre-jump repulsion due to an electrical double layer interaction arising from the charge on the pre-existing nanobubble surface [22], soft post-jump repulsion due to contact line drag on the spreading bridging nanobubble [42] and multiple steps in the pull-off force due to multiple, thin stranded, bridging nanobubbles [45]. In addition, the range of the attraction has been shown to decrease in de-aerated water or in surfaces never exposed to the atmosphere due to the nanobubbles shrinking or disappearing [20,38–41]. Optical visualisation of hydrophobic surfaces has revealed long-lived micron-sized bubbles, (kilo-nanobubbles) [6,22] and scanning probe microscopy has revealed both isolated [51] and networked [44,45] nanobubbles.

Whilst the experimental evidence conclusively shows that nanobubbles exist and are the origin of the measured long-ranged hydrophobic attractions, the theoretical understanding of the nanobubble phenomenon is not so advanced. There remain unanswered a number of questions regarding the origin and stability of nanobubbles. There is an apparent paradox between the Laplace–Young equation and the observed

occurrence and stability of nanobubbles. It is unclear whether or not the gas inside the nanobubbles is in equilibrium with that in the solution, and whether the solution is saturated or supersaturated. If it is a non-equilibrium situation, it remains to identify the impediment to achieving equilibrium and the time scales over which this occurs. Further light on these issues will hopefully be shed by well-designed experiments.

Despite these fundamental issues that await clarification, enough is now known about the nanobubble phenomenon to begin to explore the practical implications. In the context of forces one can now understand the extreme instability of lyophobic dispersions and the strong and irreversible adhesion of hydrophobic colloids. One can speculate upon the possibility of controlling the stability of such dispersions by varying the amount and type of gas supersaturation of the solution. Such long-range attractions will occur for even quite low coverages of nanobubbles. Beyond this, the films of nanobubbles revealed by the scanning probe images of Tyrrell and Attard [44,45], represent complete coverage of the hydrophobic surface, and this calls for a radically new viewpoint. In these cases, the interactions of the particle are likely more akin to bubble interactions and they ought to be treated as such. In controlling particle interactions by altering the nature of the surface by chemical reaction or by physical adsorption, consideration ought be given to the fact, that in some cases, the solid surface will be inaccessible and the properties of the liquid–vapour interface may be the most relevant one. Such nanobubble coverings also have surprising consequences for the motion of particles in liquids or the flow of liquids next to surfaces or in capillaries. One can well anticipate a reduction in drag by such a nanobubble film, since slip obviously occurs at a fluid interface whereas stick boundary conditions are traditionally invoked in the hydrodynamic flow at solid surfaces. This would appear to account for the unexpectedly high rates of flow that have been measured in hydrophobed capillaries [56], and offers a novel approach to reducing the drag on macroscopic objects moving in water.

Acknowledgments

I would like to thank John Parker, Archie Carambassis, Mark Rutland and James Tyrrell for helping to increase the understanding and to decrease the mystery of the hydrophobic attraction.

References

- [1] T.D. Blake, J.A. Kitchener, *J. Chem. Soc. Faraday Trans. 1* (68) (1972) 1435.
- [2] J.N. Israelachvili, R.M. Pashley, *J. Colloid Interface Sci.* 98 (1984) 500.
- [3] Ya I. Rabinovich, B.V. Derjaguin, *Colloids Surf.* 30 (1988) 243.
- [4] H.K. Christenson, P.M. Claesson, *Adv. Colloid Interface Sci.* 91 (2001) 391.
- [5] J.C. Eriksson, S. Ljunggren, P.M. Claesson, *J. Chem. Soc. Faraday Trans. 2* (85) (1989) 163.
- [6] R.F. Consideine, C.J. Drummond, *Langmuir* 16 (2000) 631.
- [7] P. Attard, *J. Phys. Chem.* 93 (1989) 6441.
- [8] R. Podgornik, *J. Chem. Phys.* 91 (1989) 5840.
- [9] O. Spalla, L. Belloni, *Phys. Rev. Lett.* 74 (1995) 2515.

- [10] Y.H. Tsao, D.F. Evans, H. Wennerström, *Langmuir* 9 (1993) 779.
- [11] S.J. Miklavic, D.Y.C. Chan, L.R. White, T.W. Healy, *J. Phys. Chem.* 98 (1994) 9022.
- [12] S.J. Miklavic, *J. Chem. Phys.* 103 (1995) 4794.
- [13] P.M. Claesson, C.E. Blom, P.C. Herder, B.W. Ninham, *J. Colloid Interface Sci.* 114 (1986) 234.
- [14] P.M. Claesson, H.K. Christenson, *J. Phys. Chem.* 92 (1988) 1650.
- [15] H.K. Christenson, P.M. Claesson, J. Berg, P.C. Herder, *J. Phys. Chem.* 93 (1989) 1472.
- [16] P. Kekicheff, O. Spalla, *Phys. Rev. Lett.* 75 (1995) 1851.
- [17] H.K. Christenson, J. Fang, B.W. Ninham, J.L. Parker, *J. Phys. Chem.* 94 (1990) 8004.
- [18] H.K. Christenson, P.M. Claesson, J.L. Parker, *J. Phys. Chem.* 96 (1992) 6725.
- [19] J.L. Parker, P.M. Claesson, P. Attard, *J. Phys. Chem.* 98 (1994) 8468.
- [20] J. Wood, R. Sharma, *Langmuir* 11 (1995) 4797.
- [21] V.S.J. Craig, B.W. Ninham, R.M. Pashley, *Langmuir* 14 (1998) 3326.
- [22] A. Carambassis, L.C. Jonker, P. Attard, M. Rutland, *Phys. Rev. Lett.* 80 (1998) 5357.
- [23] D.R. Berard, P. Attard, G.N. Patey, *J. Chem. Phys.* 98 (1993) 7236.
- [24] H.K. Christenson, P.M. Claesson, *Science* 239 (1988) 390.
- [25] P. Attard, C.P. Ursenbach, G.N. Patey, *Phys. Rev. A* 45 (1992) 7621.
- [26] P.G. Debenedetti, A.A. Chialvo, *J. Chem. Phys.* 97 (1992) 504.
- [27] J. Forsman, C.E. Woodward, *Mol. Phys.* 90 (1997) 637.
- [28] K. Lum, D. Chandler, *Int. J. Thermophys.* 19 (1998) 845.
- [29] K. Lum, D. Chandler, J.D. Weeks, *J. Phys. Chem. B* 103 (1999) 4570.
- [30] M.E. Fisher, P.G. de Gennes, *C. R. Acad. Sci. Paris Ser. B* 287 (1978) 207.
- [31] J.L. Cardy, *Phys. Rev. Lett.* 65 (1990) 1443.
- [32] D.W. Pohl, W.I. Goldburg, *Phys. Rev. Lett.* 48 (1982) 1111.
- [33] D. Beysens, D. Esteve, *Phys. Rev. Lett.* 54 (1985) 2123.
- [34] E.A. Boucher, *J. Chem. Soc. Faraday Trans.* 86 (1990) 2263.
- [35] P. Attard, *Langmuir* 12 (1996) 1693.
- [36] J.C. Eriksson, S. Ljunggren, *Langmuir* 11 (1995) 2325.
- [37] S. Ljunggren, J.C. Eriksson, *Colloid Surf. A* 129–130 (1997) 151.
- [38] L. Meagher, V.S.J. Craig, *Langmuir* 10 (1994) 2736.
- [39] R.F. Considine, R.A. Hayes, R.G. Horn, *Langmuir* 15 (1999) 1657.
- [40] J. Mahnke, J. Stearnes, R.A. Hayes, D. Fornasiero, J. Ralston, *Phys. Chem. Chem. Phys.* 1 (1999) 2793.
- [41] N. Ishida, M. Sakamoto, M. Miyahara, K. Higashitani, *Langmuir* 16 (2000) 5681.
- [42] P. Attard, *Langmuir* 16 (2000) 4455.
- [43] G.E. Yakubov, H.J. Butt, O.I. Vinogradova, *J. Phys. Chem. B* 104 (2000) 3407.
- [44] J.W.G. Tyrrell, P. Attard, *Phys. Rev. Lett.* 87 (2001) 176104.
- [45] J.W.G. Tyrrell, P. Attard, *Langmuir* 18 (2002) 160.
- [46] J.Y. Kim, M.G. Song, J.D. Kim, *J. Colloid Interface Sci.* 223 (2000) 285.
- [47] C. Yang, T. Dabros, D. Li, J. Czarnecki, J.H. Masliyah, *J. Colloid Interface Sci.* 243 (2001) 128.
- [48] S.J. Miklavcic, *J. Chem. Phys.* 103 (1995) 4794.
- [49] P. Attard, *J. Stat. Phys.* 100 (2000) 445.
- [50] P. Attard, *Thermodynamics and Statistical Mechanics: Equilibrium by Entropy Maximisation*, Academic Press, London, 2002.
- [51] N. Ishida, T. Inoue, M. Miyahara, K. Higashitani, *Langmuir* 16 (2000) 6377.
- [52] P. Attard, M.P. Moody, J.W.G. Tyrrell, *Physica A* 314 (2002) 696.
- [53] M.P. Moody, P. Attard, *J. Chem. Phys.* 117 (2002) 6705.
- [54] M.P. Moody, P. Attard, *J. Chem. Phys.* 115 (2001) 8967.
- [55] D.W. Oxtoby, R. Evans, *J. Chem. Phys.* 89 (1988) 7521.
- [56] T.D. Blake, *Colloids Surf.* 47 (1990) 135.